

Experimental and Theoretical Demonstration of the Interfacial Interaction Potential Between an Adsorbed Film and a Smooth Substrate

R. Mu, A. Ueda, M. H. Wu, Y. S. Tung, and D. O. Henderson*

Chemical Physics Laboratory, Department of Physics, Fisk University, Nashville, Tennessee 37208

R. T. Chamberlain, W. Curby, and A. Mercado

System Development, Aviation Security Resources, Federal Aviation Technical Center, Atlantic City International Airport, Atlantic City, New Jersey 08405

Received: September 21, 1999

The atomic force microscopy (AFM) technique has been developed to study the sublimation rate of an organic solid film on smooth surfaces. On the basis of the experimental results, a dipole-induced dipole propagation potential is employed to explain a nonlinear sublimation rate of a solid TNT thin film in a very close proximity to the substrate surface. In this model, three important physical parameters, the bulk sublimation rate δ_0 , surface interaction potential U_0 , and the effective decay length of the surface potential h_0 , are introduced without any arbitrary constants. It is argued that the model reflects a general phenomena rather than a special case.

Introduction

The study of surface potentials and adsorbate–adsorbent interactions is of great importance from both fundamental and applied science aspects. Much progress has been made to elucidate the nature of the adsorbed atoms or molecules interacting with a substrate surface in terms of wettability, two-dimensional phase transitions, and interfacial effects.¹ However, due to the complexity of this subject, much of the research has been limited to rather simple and idealized systems such as using single atoms (Ar, Xe, Kr, etc.) and/or simple molecules (CH₄, CO, C₂H₆, etc.)¹ as probes to elucidate interfacial interaction between the probe molecules and a substrate. In practice, it is very difficult and some times impossible to apply the results from a model system to real world adsorbate–adsorbent interfacial phenomena, since in most cases, the nature of the interaction depends on the properties of both a substrate surface and adsorbate atoms or molecules. This problem becomes much more pronounced when (i) an adsorbed molecule is large and has more complex structure, (ii) a substrate surface is inhomogeneous and may be contaminated, and (iii) the surface coverage of the adsorbed molecules is high enough so that a film and/or a droplet has been formed.

In this work, we have investigated the sublimation rates of a thin solid film ($d \approx 3$ nm) of 2,4,6-trinitrotoluene (TNT) on a Muscovite mica, a naturally oxidized silicon wafer, and highly oriented pyrolytic graphite (HOPG) surfaces. Both AFM and ellipsometric techniques are employed to study how the thickness d of the film changes as a function of sublimation time t . On the basis of the experimental results, a theoretical model is proposed which contains three important parameters that can be determined experimentally. They are a sublimation constant, δ_0 , reflecting a sublimation rate of the bulk material; a critical sublimation decay length, h_0 , indicating an effective range of a surface perturbation into an adsorbed thin film; and an interaction potential constant, U_0 , at the interface indicating the strength of the interaction between the film and the substrate.

Experimental Section

2,4,6-Trinitrotoluene (TNT) purchased from Chem Service with purity of 99% was used to prepare the thin films. Electronic grade silicon wafers were purchased from Virginia Semiconductor. The cut surfaces of these silicon wafers have [100] orientation. The front side is polished and the back surface remains rough. On the basis of AFM measurements, the root-mean-square (RMS) roughness of the polished silicon wafer surface is $\sim 2\text{--}3$ Å. Ellipsometry measurements indicate that the silicon surface is covered with a 15–17 Å silicon dioxide layer. To reduce the possible confusion to the reader, we will hereafter refer to *the surface of the silicon wafer* as *silica surface*. Highly oriented pyrolytic graphite (HOPG) substrates were purchased from Advanced Ceramics, and Muscovite mica was obtained from Standard Probe, Inc. (SPI). Clean graphite and mica surfaces were prepared by cleaving along the (0001) and (001) planes with an adhesive tape before the film deposition.

TNT vapor deposition was carried out with a laboratory-designed cylindrical vapor dosing chamber. The detailed procedure for preparing the films was described elsewhere.^{2,3} To prevent droplet formation and crystallization, the three substrates, silica, mica, and graphite were cooled to liquid nitrogen temperature -195 °C and the TNT source was heated to 93 °C. During the course of deposition, the entire system was maintained under helium gas purge to prevent possible water condensation. After the vapor deposition, the substrates were slowly warmed to room temperature before being subjected to both AFM and ellipsometric measurements. Under these deposition conditions, the TNT film is amorphous.

The AFM used in this study is a Nanoscope III (Digital Instruments, Santa Barbara, CA). Tapping mode AFM was employed to image the thin solid film surface under ambient conditions. The reason we used tapping mode AFM technique over the contact mode AFM is the easiness to minimize the tip–sample interactions which may lead to physical damage or

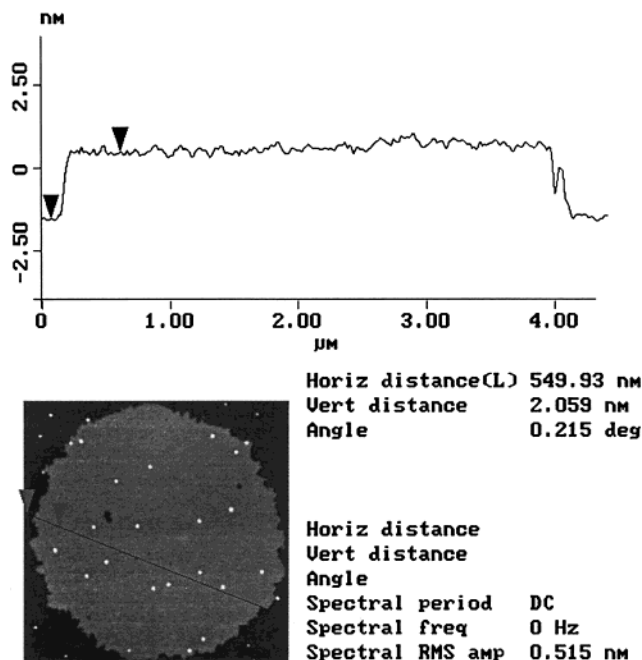


Figure 1. Tapping mode AFM images of a TNT platelet deposited on a silica surface. The image was obtained under ambient condition 15 h after preparation. The surface is smooth and the average height is $\sim 2 \pm 0.2$ nm.

modifications to the sample surface. A series of tests has been done by repeatedly scanning the same sample surface well over 50 times. Little structural modification was observed. For the AFM measurements reported in this paper, every adjacent image was acquired with a time interval of 1–3 h. Thus, the effect of surface perturbation due to the tip was negligible. A single wavelength (546 nm) Rudolf 406 ellipsometer with an incident light angle of 70° was used to obtain the film thickness.

Results and Discussion

Figure 1 illustrates a tapping mode AFM image of a solid TNT film deposited on a silica surface after 15 h sublimation

in air. The film thickness is $\sim 2 \pm 0.2$ nm. When the film thickness is larger than ~ 1 nm, the sublimation process under ambient conditions did not lead to roughening of the surface. However, when the film thickness is near and below 1 nm, the surface becomes relatively rough and some of the silica surface is exposed, which is shown in Figure 2.

It is expected that the sublimation process often results in roughening of a film surface. This has been reported in numerous cases.⁴ This roughening process has been explained in terms of solid state sublimation. That is, the sublimation usually starts at the surface defect sites, such as grain boundaries, steps, kinks, and vacancies, where the molecules have higher energy than those in the bulk. Local thermal fluctuations can provide enough thermal energy for these molecules to overcome the binding potential barriers and escape from the surface. The desorption of these molecules can further disturb the local thermal stability. As a result, a heterogeneous sublimation at the surface will give rise to the surface roughness. It is worthwhile to point out that the explanation offered above is only valid for a bulk surface. In the case of molecular film adsorbed on a surface, a perturbation from the substrate surface will modify the nature of the desorption process. In addition, the structure of the thin solid film is not necessarily the same as that of the bulk solid.

To estimate the sublimation rate of a solid TNT film (or platelet) on a surface with the AFM technique, we have first imaged a number of solid TNT platelets on a silica surface as a function of sublimation time. Then, the total volume and surface area change at a given time interval was calculated using Digital Instrument software. The sublimation rate σ_z (molecules/cm² s) can be determined from the equation

$$\sigma_z = -\frac{\rho N_o}{MA} \frac{dV(t)}{dt} \quad (1)$$

where $V(t)$ is the total volume of the platelets at time t , N_o , ρ , and M are the Avogadro constant, density, and molecular weight of TNT, and A is the measured surface area of the platelets at time t . Because of the fact that the exact density of the

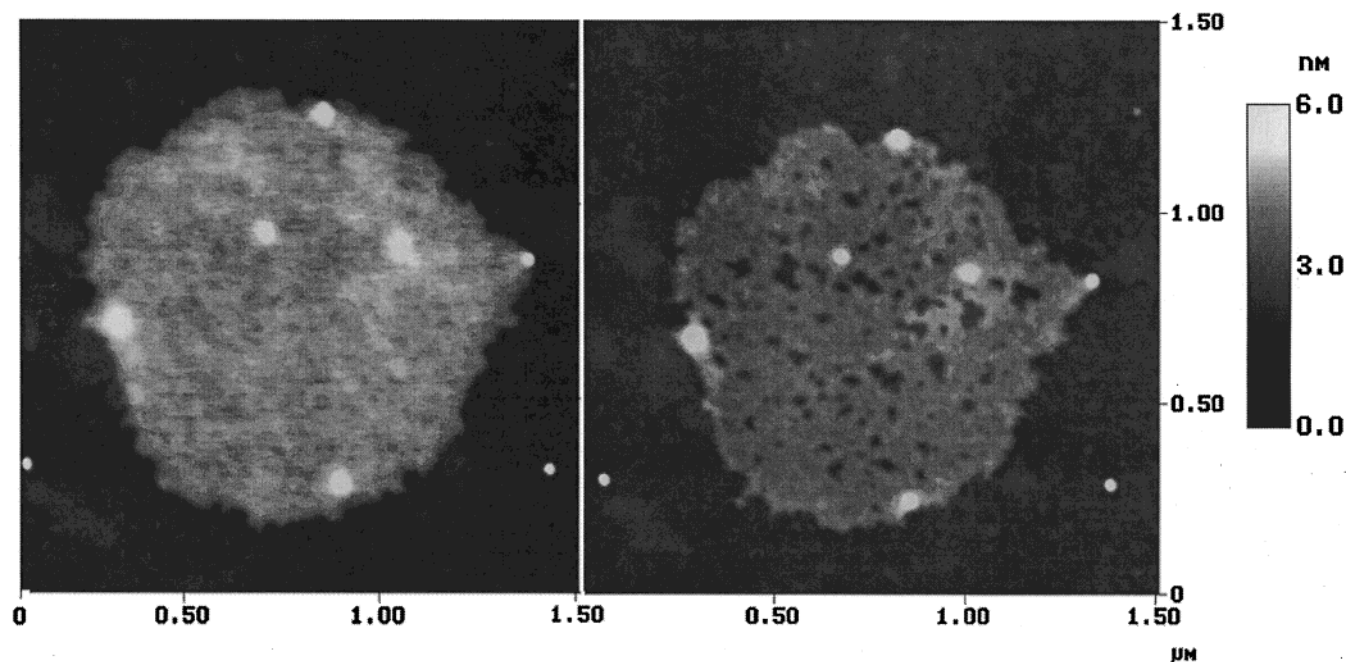


Figure 2. Tapping mode AFM images of solid TNT film on a silica surface. The image on the right was obtained in the 48 h after the image on the left. The average height on the left was $\sim 2.6 \pm 0.2$ nm, while the average height became about $\sim 1.1 \pm 0.2$ nm on the right and the surface became roughened.

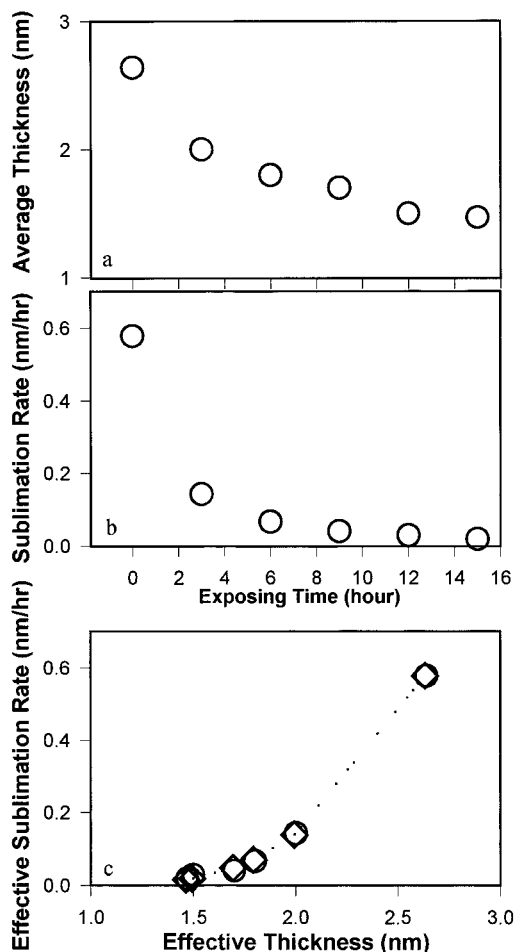


Figure 3. Experimental results to show the average height, sublimation rate change as a function of time, and the effective sublimation rate vs the average thickness of the film ((○) experimental, (◇) DPP model fitted).

amorphous TNT is not known, we have estimated the “effective sublimation rate” δ in terms of the effective thickness change of the platelets as a function of time. That is,

$$\delta = -\frac{1}{A} \frac{dV(t)}{dt} \left(\equiv \frac{\sigma M}{N_o \rho} \right) \quad (2)$$

Figure 3 shows the plots of the effective sublimation rate δ of TNT as illustrated in Figure 1 as the function of the sublimation time. Each data point represents a 3 h time interval. It is interesting to note that the measured δ is not a constant quantity as the film thickness decreases. In fact, δ shows nonlinear behavior.

Adsorption of molecules onto a surface can be a complex process.⁵ The interaction potential ranges from strong interactions via chemical bonding to weak interactions of van der Waals type. Hydrogen bonding can also play an important role in the polar molecular systems. The strength of the hydrogen bonding typically falls between the chemical bonding and van der Waals interaction.

In the TNT–silica system, there could be many types of interactions that are operative. (1) It is known that silica surface contains Si–OH groups as a result of natural oxidation under ambient conditions. Water molecules in the air can be adsorbed onto the silica surface forming hydrogen bonds with OH groups on the surface unless the substrate is heated above 450 °C under vacuum⁶. (2) A TNT molecule contains three polar NO₂ groups

and an easily polarizable benzene ring. From these considerations, both hydrogen bonding and van der Waals interactions are expected for the TNT–silica system. However, the current experimental results seem to suggest that the surface potential must be of a long-range nature. As illustrated in Figure 3, the effective range of the potential can be as far as 3 nm away from the surface. Such a range is far beyond what is expected for hydrogen bonding (2–3 Å).⁷

As discussed in great detail by Adamson,⁵ there are three different types of intermolecular forces between molecules which can be associated with long-range forces: (i) a charge–a polarizable molecule interaction; (ii) a dipole–polarizable species interaction; (iii) dispersion forces. Each type of interaction potential can be expressed as a function of an intermolecular distance d and can be generalized as follows:

$$U(d) = -C_1 d^m - C_2 d^n - C_3 d^p - \dots \quad (3)$$

where d is the intermolecular separation, C_1 , C_2 , and C_3 are the constants related to a charge, a dipole or an induced dipole, while m , n , and p are integers which reflect the nature of the interaction. For example, when $C_2 = C_3 = 0$, $n = p = 0$ and $m = -4$, $U(d)$ is the potential for a charge–a polarizable molecular interaction; for $m = -6$, the interaction is a dipole-induced dipole interaction; for $C_1 \neq C_2 \neq C_3 \neq 0$, and $m = -6$, $n = -8$, and $p = -10$, the interaction potential is a dispersion type. In this case, the first term represents dipole–dipole interaction. The second term reflects dipole–quadrupole interaction, and the third term can be the sum of the dipole–octupole and quadrupole–quadrupole interactions. We have generalized these models to fit our experimental data. A consistent deviation between the experimental results and model calculations was observed when attempts were made to do a numerical fitting with the model. The deviation becomes much more pronounced as the film thickness decreases. This has led us to the dipole-induced dipole interaction which considers the propagation of the polarization.

Consider a silica surface with a charge of q which is due to the OH groups that terminate the surface. An induced dipole moment μ_{ind} will be created upon the adsorption of a TNT molecule on silica surface. The value of the induced dipole μ_{ind} is proportional to the electric field E at the adsorption site, i.e., $\mu_{\text{ind}} = \alpha E$, where α is the molecular polarizability. Therefore, the interaction potential between the first layer of the TNT molecules and the silica substrate surface $U_{0,1}$ is

$$U_{0,1}(d) = -\frac{\alpha q^2}{2d^4} = \left[\frac{1}{2} \right] \left[\frac{q}{d} \right] \left[\frac{\alpha q}{d^3} \right] \quad (4)$$

Similarly, the interaction potential between the first layer and the second layer is

$$U_{1,2}(d) = \left[\frac{1}{2} \right] \left[\frac{q}{d} \right] \left[\frac{\alpha q}{d^3} \right] \left[\left(\frac{\alpha}{d^3} \right)^2 \right] = U_{0,1}(d) \left[\frac{\alpha}{d^3} \right]^2 \quad (5)$$

A generalized layer-by-layer interaction propagation is then

$$U_{i,i+1}(d) = U_{i-1,i}(d) \left[\frac{\alpha}{d^3} \right]^2 \quad (6)$$

Therefore, the locus of this successive value for the dipole-induced dipole propagation interaction potential is

$$U(h(t)) = U_o e^{-(h(t)/h_o)} \quad (7)$$

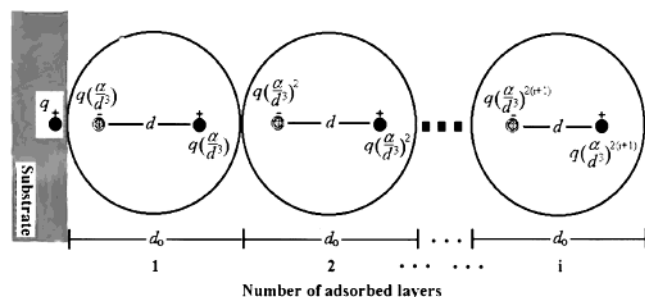


Figure 4. Model sketch to demonstrate a long-range interaction potential through a dipole-induced dipole propagation polarization (DPP) in the adsorbed thin film.

where $h_0 \equiv [-d_0/\ln(\alpha/d^3)]$, h is the distance from a substrate surface or film thickness. U_0 is the maximum interaction potential close to the adsorbent–substrate interface. d_0 is the size of an adsorbed molecule, and d is an equivalent separation of the induced charges as illustrated in Figure 4.

By combining eqs 2 and 7, the effective sublimation rate δ can be written as

$$\delta(h(t_i)) = \delta_0 \exp\left(-\frac{U(h(t_i))}{kT}\right) \quad (8)$$

The final form of the effective sublimation rate as a function of the film thickness becomes

$$\delta(h(t_i)) = \delta_0 \exp\left(-\frac{1}{kT}\left[U_0 \exp\left(-\frac{h(t_i)}{h_0}\right)\right]\right) \quad (9)$$

There are three fundamental parameters contained in this model: the TNT–silica surface interaction potential constant, U_0 , a critical decay length, h_0 , and a bulk sublimation rate, δ_0 , of solid TNT. T and k are the sublimation temperature and Boltzman constant. Both $\delta(h(t_i))$ and $h(t_i)$ are the measured time-dependent sublimation rate and the thickness of a platelet. They are plotted with sublimation time in parts a and b of Figure 3. Figure 3c shows both the experimentally determined $h(t)$ vs $\delta(t)$ plot along with the model fitted data based on eq 8. It is clear that this model gives an excellent fitting as compared to the other models considered.⁵ On the basis of the model fitting we determined (i) the sublimation rate constant δ_0 is ~ 2.7 nm/h, reflecting a sublimation rate of bulk TNT at ambient conditions; (ii) the critical decay length h_0 is ~ 1 nm, indicating that the perturbation from silica surface extends up to the nanometer range, that is, TNT molecules at ~ 1 nm away from a silica surface can experience the surface forces; (iii) the surface potential for TNT molecules at silica surface is ~ 57 kJ/mol.

In addition to the physical parameter which provides direct physical significance, such as δ_0 , the bulk TNT sublimation rate, other indirect physical implications of TNT molecules near silica surface have been revealed. Because of the fact that the critical decay length h_0 is on the order of a nanometer, it suggests that the TNT–silica surface interaction is via a long-range force. Any direct intermolecular interactions, such as covalent and hydrogen bonding, fall in 0.1–0.2 nm range. Since the experimental data can be best fitted with the potential of an exponential type, the nature of the TNT–silica surface interaction can be described by a dipole-induced dipole moment propagation potential. It should be pointed out that the proposed surface potential function in the present case is only a part of the total interaction potential for the TNT molecules on the silica surface. That is, the total interaction potential for a TNT molecule at distance h consists of a surface potential $U(h)$ and

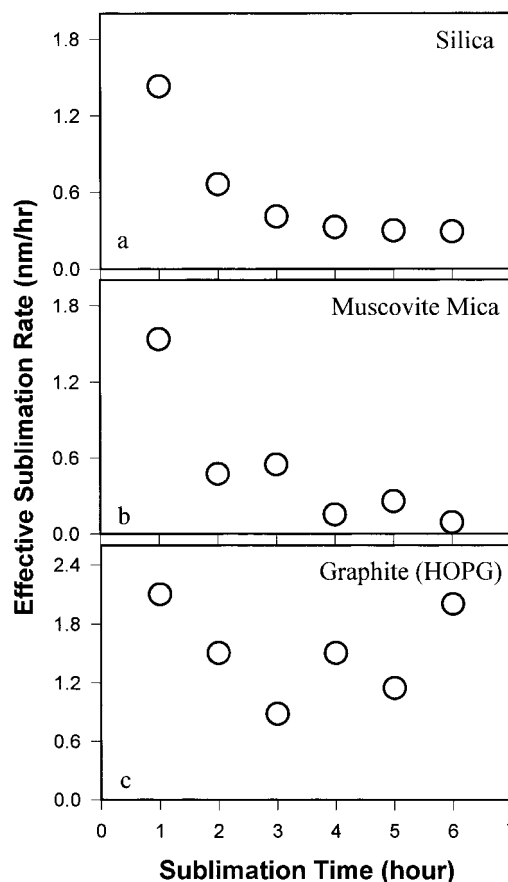


Figure 5. Measured sublimation rates of TNT film on silica, Muscovite mica, and graphite (HOPG) surfaces as a function of time via ellipsometry.

an intermolecular interaction potential U_H , which includes hydrogen bonding and van der Waals forces between neighboring molecules. It is known that the intermolecular interaction potential for TNT molecules in the solid phase is stronger than that of TNT–surface interaction. A TNT sublimation study by Cundall et al.⁸ suggests that the enthalpy change for TNT sublimation at room temperature (25 °C) is 113.2 ± 1.5 kJ/mol, while the maximum surface potential U_0 obtained at present is ~ 57 kJ/mol. This would seem to suggest that the sublimation rate is dominated by the intermolecular potential of neighboring TNT molecules. However, as the thickness of the film decreases, the interaction potential between the TNT film increases and therefore the total potential $U(h) + U_H$ also increases. This increase in the total potential can account for the decreasing sublimation rate as the film thickness decreases.

Figure 5 illustrates the effective sublimation rates of TNT on three different surfaces. Figure 5a shows the sublimation rate of submicrometer sized TNT particles on a silica surface. Parts b and c of Figure 5 exemplify the sublimation rates of micrometer sized TNT on mica and graphite surfaces measured with an AFM. The results also suggest a strong surface effect on mica when the particle size of the TNT is in the nanometer and micrometer range. The measured sublimation rate for these submicron TNT particles is very similar to the rate for TNT platelets on silica. This observation implies that the same model used earlier is still valid for the particle size much smaller than micrometer size. However, due to the irregular shape of these TNT particles and extensive surface roughness, no attempts were made to do a quantitative analysis.

Tapping mode AFM measurements of TNT deposited on three substrates indicate that rate is nonlinear for TNT on mica

and silica, but such behavior is not apparent for TNT on graphite. It is known that the surface ending group of mica in the basal cleavage plane is a hexagonal lattice structure consisting of SiO_4 tetrahedra with a periodicity of 0.52 nm.¹⁰ From this perspective, the surface chemistry of mica is very much like an oxidized silicon surface. Consequently, it is expected that sublimation characteristics for TNT on mica and silica surfaces should be similar. On the other hand, the nature of TNT-graphite interaction is of the van der Waals type. Because the TNT-graphite interactions are relatively weak, they have little effect on the sublimation rate, i.e., it is linear.

As reported by Tung et al.,² the sublimation rates measured by ellipsometry show reasonable agreement with those obtained by the AFM technique for thick TNT films on surfaces. Unfortunately, this technique fails to reveal the nonlinear behavior of the sublimation rate as TNT molecules are near silica or mica surfaces. The lack of the nonlinear sublimation rates as determined by ellipsometry most likely originates from the large sampling area ($\sim 0.3 \text{ cm}^2$) as compared to the nanometer range measured by AFM. Within such a large area, there are hundreds of thousands of TNT particles with different shapes and sizes at different stages of sublimation, which gives rise to an average value as compared to the AFM measurements that render the sublimation dynamics of an individual particle that would exhibit a nonlinear behavior due to interfacial interactions. For example, the sublimation rate measured by ellipsometry for TNT on silica surface is $\sim 1 \text{ nm/h}$. This value falls between sublimation rates obtained for bulk and for TNT molecules near a silica surface with the AFM technique. This is due to the fact that ellipsometry samples an ensemble of many TNT particles on silica surface at various sublimation stages. The larger particles give the bulk sublimation rate, while the smaller ones give a lower sublimation rate due to the surface interaction potential. Therefore, for a high surface coverage, the average value is expected to be between the sublimation rates of bulk and the thin film on a silica surface. This is in good agreement with ellipsometry measurements. In addition, the silica surface with no TNT particles gives zero contribution to the sublimation rate which also lowers the effective sublimation rate over the sampling area.

It is also worthwhile to consider supercooling effects on small particles. In the case of a surface adsorbed molecular system, the thermodynamics are also perturbed by the substrate. For both TNT and PETN explosives, for example, micron-sized liquid droplets are routinely observed when they are deposited on silica, mica, and graphite surfaces. These droplets are fairly stable under ambient conditions. It takes hours and sometimes

days for these droplets to crystallize. The growth dynamics of a large cluster is diffusion-limited aggregation and can account for the "slow" crystallization.² The study of the evaporation rate of these liquid droplets is critical for understanding the thermodynamics of these supercooled droplets on a surface. Both theoretical modeling and experimental evaluation of the evaporation rate for liquid droplets are currently underway and will be published separately.

Conclusion

We have coupled both AFM techniques with theoretical modeling to study the sublimation rate of a TNT solid film on silica and mica surfaces. For the first time, we are able to measure the sublimation rate with high accuracy. A theoretical model has been developed with no arbitrary constants. This model provides not only information on the nature of the thin film-substrate interaction, i.e., dipole-induced dipole propagation interaction, but also renders three important physical parameters. They are the bulk TNT sublimation rate, δ_o , the maximum surface interaction potential, U_o , and the effective range of the surface potential, h_o .

Acknowledgment. This work was supported by the Federal Aviation Administrations under Grant 93-G-057.

References and Notes

- (1) For example, see: Steele, W. *Chem. Rev.* **1993**, 93, 2355. Vold, R. D.; Vold, M. J. *Colloid and Interface Chemistry*; Addison and Wesley: Reading, MA, 1983; Chapter 3. Zink, J. C.; Reif, J.; Matthias, E. *Phys. Rev. Lett.* **1992**, 68, 3595. Sullivan, D. E. *Faraday Symp. Chem. Soc.* **1981**, 16, 191. Dietrich, S. In *Phase Transitions and Critical Phenomena*; Domb, C., Lebowitz, J. L., Eds.; Academic Press: New York, 1988; Vol. 12, Chapter 1.
- (2) Tung, Y. S.; Mu, R.; Ueda, A.; Henderson, D. O.; Curby, W.; Mercado, A. *Scanning*, in press.
- (3) Henderson, D. O.; George, M. A.; Burger, A.; Mu, R.; Hu, Z.; Houston, G. C. *Scanning Microsc.* **1995**, 9, 387.
- (4) Tanaka, H.; Koga, N.; Galway, A. K. *J. Chem. Educ.* **1995**, 72, 251.
- (5) Adamson, A. W. *Physical Chemistry of Surfaces*, 4th ed.; John Wiley & Sons: New York, 1982; Chapter VI, pp 249.
- (6) Morrow, B. A.; McFarlan, A. J. *J. Phys. Chem.* **1992**, 96, 1395. Mu, R.; Malhotra, R. *Phys. Rev. B* **1991**, 44, 4296. Shen, J. H.; Kiler, K. *J. Colloid Interface Sci.* **1980**, 75, 56.
- (7) Pimentel, G. C.; Sederholm, C. H. *J. Chem. Phys.* **1956**, 24, 639. Hadzi, D.; Bratos, S. In *The Hydrogen Bond*; Schuster, P., Zundel, G., Sandorby, C., Eds.; Amsterdam, New York, 1976; Vol. II, Chapter 12.
- (8) Cundall, R. B.; Palmer, T. F.; Wood, C. E. C. *J. Chem. Soc., Faraday Trans. 1* **1978**, 74, 1339.
- (9) Mu, R.; Xue, Y.; Henderson, D. O.; Frazier, D. O. *Phys. Rev. B* **1996**, 53, 6041.
- (10) Miyake, S. *Appl. Phys. Lett.* **1994**, 65, 980.